

Emission of acoustic phonons due to tunnel relaxation of nonequilibrium electrons in double quantum wells

F. T. Vasko and O. G. Balev

Institute of Semiconductors, Academy of Sciences, Prospekt Nauky 45, Kiev 252650, Ukraine

P. Vasilopoulos

Department of Physics, Concordia University, 1455 de Maisonneuve Boulevard West, Montréal, Canada H3G 1M8

(Received 14 December 1992)

Emission of nonequilibrium acoustic phonons due to electron tunneling in double-quantum-well structures is considered. The energy and angular dependences of the nonequilibrium phonon distribution are studied for interwell transitions and the differences with those for intrawell transitions are pointed out. Due to the interwell interference the energy and angular distributions of the emitted phonons are strongly nonmonotonic. The intensity of the high-energy phonon flow due to interwell transitions is evaluated; for degenerate electrons its value is substantially larger than the intensity of phonon flow caused by the usual process while for nondegenerate hot electrons these two intensities can have comparable values.

I. INTRODUCTION

Acoustic-phonon emission by hot two-dimensional (2D) electrons in metal-insulator-semiconductor structures, selectively doped heterojunctions, and quantum wells has been investigated in detail.¹⁻³ The energy and angular distributions of the emitted phonons were studied also in the presence of magnetic field applied perpendicular to the 2D plane (cf. Ref. 3 and references cited therein). In this paper we obtain the nonequilibrium distribution of acoustic phonons that are emitted by electrons in the process of tunneling-assisted relaxation in double-quantum-well (DQW) structures. The electron distribution is supposed to be a nonequilibrium one; in this case it is impossible to determine the characteristics of phonon emission with the usual thermodynamic methods that use blackbody-type formulas. Electron tunnel relaxation in such structures determines real-space transfer processes, related with electron tunneling between quantum wells (QW's), which could be important for applications.⁴ Straightforward investigations of the tunneling process in DQW structures were carried out with the help of high time-resolution photoluminescence techniques.⁵ Observation of the acoustic-phonon emission generated by interwell tunnel transitions also is of obvious interest for studies of such tunneling processes. Moreover, the flow of phonons, emitted during these transitions, can be sufficiently intense and their energy distribution can be appreciably modified under the shift of tunnel-connected levels which results when a transverse electric field is applied to the DQW structure.

We consider a simple DQW structure as shown in Fig. 1. Here we are treating the case when only the two lowest tunnel-connected levels are occupied. We consider only the transitions between these states due to emission of acoustic phonons (absorption can be neglected for the conditions stated below). If the levels are out of resonance the wave function of one of them is mainly

concentrated in the left (*l*) QW and that of the other in the right (*r*) QW. We assume that the nonequilibrium electron concentrations n_r and n_l for the *r* and *l* QW, respectively, are known and use quasiequilibrium distributions in both QW's. Such a situation arises (i) due to stationary (or impulse) photoexcitation of electron-hole pairs; (ii) when the electrons are heated by an applied longitudinal electric field that modifies their temperature as well as their concentrations n_l and n_r ; (iii) due to an abrupt imposition of a transverse voltage or a periodic square-pulse signal. The treatment given below for constant n_l and n_r can be used to describe time-dependent processes if the typical frequency of the emitted phonons exceeds the rate of electron tunnel relaxation in a DQW structure and the typical frequency of the driving signal, e.g., impulse or meander.

The energy and angular distributions of the acoustic phonons, emitted during transitions in which the quantum number that characterizes the tunnel-connected state does not change (intrawell transitions), are appreciably different from those resulting from transitions in

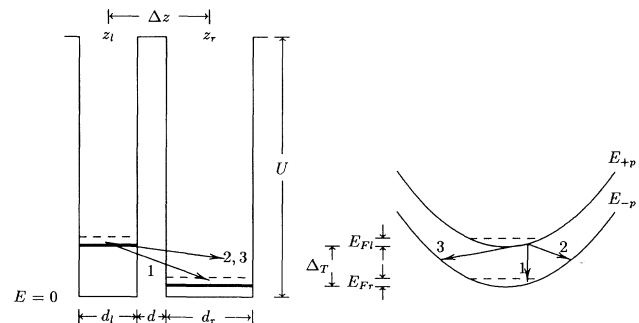


FIG. 1. Energy-band diagram and scheme of transitions for acoustic-phonon emission processes in the tunnel-connected quantum wells. Transition 1 corresponds to $\theta \approx 0$; transitions 2 and 3 correspond to $\theta \approx \pi/2$.

which this quantum number changes (interwell transitions). For intrawell transitions, discussed in Refs. 1–3 and 6, the phonon distribution depends on the average value of the longitudinal momentum of the 2D electrons which is determined by their temperature or their concentration and by the matrix element of the electron-phonon interaction in the l or r QW. For interwell transitions studied here the position of the phonon distribution maximum is determined by the energy splitting between the tunnel-connected levels Δ and the angle (with respect to the normal to the 2D plane) by which they are emitted. Strong angular dependence of the phonon distribution maximum position follows from energy and longitudinal momentum conservation conditions that accompany the emission process. In the case of emission of acoustic-phonon modes propagating almost perpendicular to the plane of the DQW structure the electron momentum is almost unchanged under interwell transitions, so that the energy of the emitted phonons will be close to Δ (transition 1 in Fig. 1). For acoustic-phonon modes propagating almost along the 2D plane under interwell transitions, the longitudinal momentum changes approximately by $\sqrt{2m^*}\Delta$, where m^* is the electron effective mass, assumed to be the same in both QW's and in the barrier region, so that the energy of the emitted phonons is of the order of the characteristic energy $E_m = \sqrt{2m^*}s^2\Delta$ (transitions 2 and 3 in Fig. 1), where s is the sound velocity. This is much smaller than Δ , if the DQW structure levels are out of resonance.

The above peculiarities of the contribution by interwell transitions to the phonon distribution are the subject of this paper. In Secs. II and III we present the formalism. In Sec. IV we treat the energy dependences of the differential acoustic energy flow for a set of angles. In Sec. V we calculate the angular dependences of the integral acoustic energy flow and the dependences of the total acoustic energy flow on Δ . In Sec. VI we present a discussion and concluding remarks.

II. BASIC RELATIONS

We begin by considering the basic relations that describe acoustic-phonon emission by nonequilibrium 2D electrons. We follow the approach developed in Ref. 6 in which the distribution function $N(\mathbf{q}, \mathbf{r})$ for acoustic phonons of wave vector $\mathbf{q} = (\mathbf{q}_{\parallel}, q_z)$ is obtained from the kinetic equation without electron contribution,

$$\left(\frac{\partial}{\partial t} + \mathbf{v}_{\mathbf{q}} \nabla_{\mathbf{r}} \right) N(\mathbf{q}, \mathbf{r}) = J_R, \quad (1)$$

where J_R is the collision integral and $\mathbf{v}_{\mathbf{q}} = \nabla_{\mathbf{q}} \omega_{\mathbf{q}}$ the phonon group velocity. Equation (1) is supplemented by the boundary condition

$$v_z [N(\mathbf{q}, d_t/2) - N(\mathbf{q}, -d_t/2)] = I(\mathbf{q}), \quad d_t \rightarrow 0; \quad (2)$$

$I(\mathbf{q})$ determines the speed of acoustic-phonon emission under relaxation of 2D electrons in a DQW of total thickness d_t and situated near the plane $z = 0$. The collision integral J_R describes relaxation processes of the emitted

phonons as they are scattered outside the 2D electron layer and v_z is the z component of their velocity. In what follows we assume the linear relation $\omega_{\mathbf{q}} = sq$ for the phonon frequency $\omega_{\mathbf{q}}$. The boundary condition (2) does not take into account absorption of acoustic phonons by 2D electrons of the DQW structure. This is valid for $\hbar\bar{\omega}_{\mathbf{q}} > k_B T_L$, where T_L is the lattice temperature and $\bar{\omega}_{\mathbf{q}}$ is a typical phonon frequency.

The right part of Eq. (2) is the speed of acoustic-phonon emission; it is given by

$$I(\mathbf{q}) = \frac{4\pi V}{\hbar} |C_q|^2 \sum_{j_1 j_2 \mathbf{p}} f_{j_1 \mathbf{p}} (1 - f_{j_2 \mathbf{p} - \hbar \mathbf{q}_{\parallel}}) |(j_1 | e^{iq_z z} | j_2)|^2 \times \delta(\hbar\omega_{\mathbf{q}} - E_{j_1 \mathbf{p}} + E_{j_2 \mathbf{p} - \hbar \mathbf{q}_{\parallel}}). \quad (3)$$

Here the transitions between the tunnel-connected electron states $|j\mathbf{p}\rangle$ of the DQW are described using the ‘‘golden rule,’’ V is the volume, and C_q measures the strength of the interaction of electrons with longitudinal acoustic-phonon modes. Further, $f_{j\mathbf{p}}$ is the occupation number of electron states with longitudinal momentum \mathbf{p} and energy $E_{j\mathbf{p}}$. The eigenvalues $E_{j\mathbf{p}}$ and eigenfunctions $|j\mathbf{p}\rangle$ can be obtained from the one-electron eigenvalue problem $H|j\mathbf{p}\rangle = E_{j\mathbf{p}}|j\mathbf{p}\rangle$ studied in Refs. 7 and 8 and discussed in the next section.

The density of energy flow \mathbf{G} due to acoustic-phonon emission is determined by the usual relation⁹

$$\mathbf{G} = (1/8\pi^3) \int d^3q \mathbf{v}_{\mathbf{q}} \hbar\omega_{\mathbf{q}} N(\mathbf{q}, \mathbf{r}). \quad (4)$$

We suppose that the transverse dimension of the sample L_z is smaller than the phonon relaxation length in the bulk (determined by J_R) but greater than the lateral dimensions of the DQW. Then in Eq. (4) we have to substitute the steady-state solution of Eq. (1) with zero on the right-hand side for which the boundary condition (2) is established on the surface of the DQW structure with area equal to S . Further, we will suppose that $N(\mathbf{q}, \mathbf{r})$ is zero on the other side of the $z = 0$ plane (see Fig. 2). Such a boundary condition, which does not take into account edge effects and diffraction under phonons emission, gives a simple stationary distribution

$$N(\mathbf{q}, \mathbf{r}) = F_{\mathbf{q}}(x - q_x z/q_z, y - q_y z/q_z), \quad (5)$$

where

$$F_{\mathbf{q}}(x, y) = \frac{q}{sq_z} I(\mathbf{q}), \quad x, y \in S. \quad (6)$$

For all other values of x and y we have $F_{\mathbf{q}}(x, y) = 0$. For definiteness we will consider the right hemisphere in Fig. 2(a). Substituting Eq. (5) in (4) we can evaluate an energy flow density in the far zone $R \gg \sqrt{S}$, where R is the distance between the observation point and the DQW structure. Then the tangential components of \mathbf{G} vanish and the radial component G_r , describing the energy flow, per unit solid angle Ω , in the direction given by the angles θ and ϕ , is independent of the lateral form of the DQW. It turns out that G_r is independent of ϕ ; it is given by

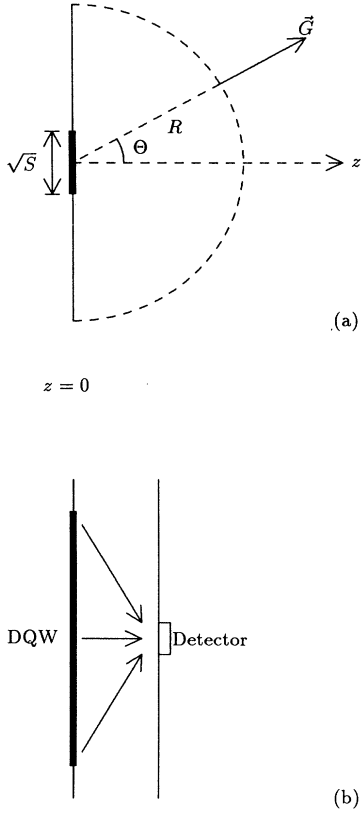


FIG. 2. Introduction of far zone, for the calculations of energy flow of acoustic phonons, from the DQW structure area on the $z = 0$ surface.

$$G_r = \frac{S}{8\pi^3 s^3 R^2} \int_0^\infty \hbar \omega^3 I(\omega, \theta) d\omega. \quad (7)$$

Rewriting the integrand on the right-hand side as *differential acoustic flow* $d^2G/d\omega d\Omega \equiv \delta G$, i.e., energy flow per unit solid angle, area, and frequency interval, we have the result

$$\delta G = \frac{\hbar \omega^3}{8\pi^3 s^3} I(\omega, \theta) \quad (8)$$

that is directly determined through the speed of phonon emission, cf. Eq. (3). The corresponding *emission intensity* is given by

$$\frac{dG}{d\Omega} = \int_0^\infty \delta G d\omega. \quad (9)$$

In the opposite limit $R \ll \sqrt{S}$ [see Fig. 2(b)], i.e., when the observation point is close to the DQW plane but far away from the edges of this plane, we obtain

$$N(\mathbf{q}) = I(\mathbf{q})/v_z, \quad (10)$$

which, being independent of r , describes the energetic and angular characteristics of the emitted phonons; here $v_z > 0$ and from Eq. (2) we have $N(\mathbf{q}) = N(\mathbf{q}, d_t/2)$ and $N(\mathbf{q}, -d_t/2) = 0$. The only nonvanishing component of

the total density of energy flow is G_z , i.e., along the z direction; it is given by

$$G_z = (1/8\pi^3) \int d^3q \hbar \omega_q I(\mathbf{q}). \quad (11)$$

Note that Eq. (11) could also be obtained from Eq. (8) (so G_z gives the density of total energy flow per unit area). Equation (11) can be given in the form

$$G_z = \int_0^\infty d\omega \int_0^{\pi/2} d\theta \sin \theta \int_0^{2\pi} d\phi \delta G. \quad (12)$$

From Eqs. (8) and (11) we see that G_z is also equal to the total energy flow per unit area of the DQW. This limit corresponds to acoustic-phonon emission out of the DQW in samples with thickness much smaller than \sqrt{S} . We denote G_z as the *total acoustic energy flow*.

III. ELECTRON STATES AND ELECTRON-PHONON INTERACTION IN A DQW STRUCTURE

Here we obtain the electron eigenfunctions and eigenvalues and also the matrix elements for transitions that appear in Eq. (3). For a pair of tunnel-connected closely located levels, formed from the ground states of the l and r *isolated* QW's, we can take the solution as a linear combination of these states, i.e., as $|\pm\rangle = \Psi_{l\mathbf{p}}^\pm |l\rangle + \Psi_{r\mathbf{p}}^\pm |r\rangle$. The orbitals $|l\rangle$ and $|r\rangle$ are exponentially decaying outside the corresponding quantum wells on the scale of $\kappa^{-1} \cong \hbar/\sqrt{2m^*U}$ where U is the band offset at the heterojunction. Denoting the width of each well by d_i , $i = l, r$ and the width of the barrier by d , cf. Fig. 1, these orbitals are given approximately by

$$|i\rangle = N_i \begin{cases} (k_i/\kappa) e^{\kappa(z-z_i+d_i/2)}, & z < z_i - d_i/2 \\ \cos[k_i(z-z_i)], & |z-z_i| < d_i/2 \\ (k_i/\kappa) e^{-\kappa(z-z_i-d_i/2)}, & z > z_i + d_i/2, \end{cases} \quad (13)$$

where N_i is a normalization factor. For small barrier penetration that we assume, i.e., for $\exp(-2\kappa d) \ll 1$ and $\kappa d_i \gg \pi$ we have $N_i \approx \sqrt{2/d_i}$ and $k_i \approx \pi/d_i$. The column of coefficients $\Psi_{l\mathbf{p}}$ and $\Psi_{r\mathbf{p}}$ satisfies the Schrödinger equation for a two-level system. Solving it we obtain the eigenfunctions $|+\rangle$ and $|-\rangle$ in the form

$$|+\rangle = N\{|l\rangle \pm [2T/(\Delta_T + \Delta)]|r\rangle\}, \quad (14a)$$

$$|-\rangle = N\{|r\rangle - [2T/(\Delta_T + \Delta)]|l\rangle\}, \quad (14b)$$

where

$$T \approx (2\pi^2 \hbar^2 / m^* \kappa d_l^3 / 2 d_r^3 / 2) e^{-\kappa d} \quad (15)$$

is the tunnel matrix element. Here $\Delta_T = \sqrt{\Delta^2 + 4T^2}$ is the level splitting with account taken of the splitting due to tunneling. For simplicity in the other sections we usually give the analytical expressions for $\Delta^2 \gg 4T^2$ and hence $\Delta_T \cong \Delta$. The normalization factor N is given by

$$N = \sqrt{(\Delta + \Delta_T)/2\Delta_T} \quad (16)$$

and the energy $E_{\pm\mathbf{p}}$ of the $|\pm\rangle$ states by

$$E_{\pm\mathbf{p}} = p^2/2m^* \pm \Delta_T/2; \quad (17)$$

the energy $E_{\pm\mathbf{p}}$ is counted from the midpoint between the left and right levels. For the potential profile given in Fig. 1 the splitting between deep levels is given approximately by $\Delta \approx (\pi^2 \hbar^2/2m^*)[d_l^{-2} - d_r^{-2}]$ if $\Delta \ll U$. It is readily seen that if $\Delta \gg T$ the $|+\rangle$ state is mainly concentrated in the left well and the $|-\rangle$ state in the right well.

Considering acoustic-phonon interaction with electron states, described by the wave functions (13) and (14), we obtain the factor that gives the mixing of $|\pm, \mathbf{p}\rangle$ states ($j, j' \equiv \pm$)

$$\langle j\mathbf{p}|e^{i\mathbf{q}\cdot\mathbf{r}}|j'\mathbf{p}'\rangle = \delta_{\mathbf{p},\mathbf{p}'+\hbar\mathbf{q}_{\parallel}} \sum_{i=l,r} \Psi_i^j \Psi_i^{j'} \langle i|e^{iq_z z}|i\rangle \quad (18)$$

which can be calculated without taking barrier penetration of the $|l\rangle$ and $|r\rangle$ orbitals into account, i.e., using Eq. (13) for $\kappa \rightarrow \infty$. The column of coefficients Ψ_l^{\pm} and Ψ_r^{\pm} in Eq. (18) can be taken from Eq. (14). The contributions containing the transverse wave-vector component q_z in Eq. (18) can be evaluated in the manner of Ref. 10 where electron scattering by phonons in a single quantum well was considered. The result is

$$\langle j|e^{iq_z z}|j\rangle e^{iq_z z_j} \chi(q_z d_j), \quad (19)$$

where

$$\chi(a) = (2/a) \sin(a/2)/[1 - (a/2\pi)^2]. \quad (20)$$

It should be noted that a finite value of Eq. (18) for $j \neq j'$ is obtained because the factors (19) in the l and r wells are different [zero value is obtained for $q_z \rightarrow 0$ due to the orthogonality of the $|+\rangle$ and $|-\rangle$ vectors]. From Eq. (18) we have

$$\begin{aligned} |(-|e^{iq_z z}|+)\rangle|^2 &= \{ \chi^2(q_z d_l) + \chi^2(q_z d_r) \\ &\quad - 2 \cos(q_z \Delta z) \chi(q_z d_l) \chi(q_z d_r) \} \\ &\quad \times \frac{4T^2(\Delta_T + \Delta)^2}{[4T^2 + (\Delta_T + \Delta)^2]^2}, \end{aligned} \quad (21)$$

where $\Delta z = z_r - z_l = (d_l + d_r)/2 + d$ is the interwell distance.

IV. ENERGY DEPENDENCES OF DIFFERENTIAL ACOUSTIC FLOW FROM A DQW

Using Eqs. (17) and (21) we can calculate the contribution of interwell transitions to the energy and angular dependences of the speed of phonon emission [cf. Eq. (3)] and to the differential acoustic flow δG or emission intensity $dG/d\Omega$, cf. Eqs. (8) and (9). This contribution is related with the terms $j_1 \neq j_2$; in our numerical calculations we will use ordinary parameters of GaAs/Al_xGa_{1-x}As structures. In this section we will study the differential acoustic flow given by Eq. (8). The integration in Eq. (3) is carried out using the condition of energy conservation and the isotropy of the problem in the plane of the 2D layer; any possible anisotropy of the electron distribution because of their drift, under heat-

ing induced by a longitudinal applied electric field, is neglected. If the average energies \bar{E}_+ and \bar{E}_- of the carriers in the $|+\rangle$ and $|-\rangle$ states, respectively, satisfy the inequality $\bar{E}_- \ll \Delta + \bar{E}_+$, in the nondegenerate case, or $\Delta + \bar{E}_+ - \bar{E}_- \gg k_B T_e$, in the degenerate case, where T_e is the electron temperature assumed the same for $|+\rangle$ and $|-\rangle$ states, then phonon emission is possible only for transitions from the $|+\rangle$ state to the $|-\rangle$ state and the contribution to $(\delta G)^{\text{inter}}$ is given only by one interwell term. Notice that for large emission angles θ the typical phonon energy diminishes with increasing θ and the phonon distribution is narrow if $\bar{E}_+ \ll \Delta$. These properties are related with the momentum and energy conservation conditions. From the latter we see that, for small q_z , the minimum and maximum wave vectors of the emitted phonons are given approximately by (see Fig. 1 where q_{\min} corresponds to transition 2 and q_{\max} corresponds to transition 3)

$$q_{\min} = \sqrt{2m^* \Delta + \bar{p}^2}/\hbar, \quad q_{\max} = q_{\min} + \bar{p}/\hbar. \quad (22)$$

Here we have assumed $\bar{p} \approx \sqrt{2m^* \bar{E}_+} \ll \sqrt{2m^* \Delta}$; this is the condition that gives a narrow energy distribution. Besides, for $q_z \rightarrow 0$ the matrix element for interwell transitions (21) goes to zero, i.e., the differential acoustic flow from the DQW goes to zero as $\theta \rightarrow \pi/2$. For $\theta \rightarrow 0$ the typical energy of the emitted acoustic phonons tends to Δ , if the restrictions for transitions to filled states of the r QW are not essential (as, e.g., in the nondegenerate case or in a degenerate case with quasi-Fermi-energies obeying $E_{Fl} \geq E_{Fr}$), and the width of the energy distribution tends to zero linearly with θ .

The exact energy and angular dependences for $(\delta G)^{\text{inter}}$ are obtained by substituting Eqs. (3) and (21) in Eq. (8). The resulting expressions are rather cumbersome for intermediate angles and strongly degenerate or nondegenerate electrons in a DQW structure. We do not discuss the intermediate case of weakly degenerate electrons since we are interested in typical characteristics of the emitted phonons that involve large angles. As discussed partly above this could be realized in a rather wide region. In this case we obtain

$$\sin \theta \gg \sqrt{2m^* s^2/\Delta}; \quad (23)$$

for many angles we cannot neglect either the oscillations of the overlap factor (21) or its monotonic strong decrease for $q_z d_{l,r} \geq 2\pi$. The oscillations of this factor are substantial if the condition

$$q_z d_{l,r} \ll 1 \quad (24)$$

is not fulfilled in which case they give an additional structure to the spectral and angular phonon distributions. In detail the result depends considerably on the parameters of the structure. If the condition (24) is fulfilled then using $q_z \Delta z \ll 1$, which is satisfied for reasonable values of d , we obtain from Eq. (21) the result

$$|(-|e^{iq_z z}|+)\rangle|^2 \approx (T/\Delta)^2 (q_z \Delta z)^2. \quad (25)$$

For $(\delta G)^{\text{inter}}$, under conditions (23) and (24), we obtain the simple expressions¹¹

$$(\delta G)_{B,F}^{\text{inter}} = \frac{\cos^2 \theta}{\sin^6 \theta} \left(\begin{array}{c} G_B \exp \left[-\frac{\Delta}{k_B T_{el}} \frac{(\omega - \omega_\theta)^2}{\omega_\theta^2} \right] \\ G_F \left[\left(\frac{\omega - \omega_\theta}{\omega_\theta} \sqrt{\frac{\Delta}{E_{Fl}}} + 1 \right) \left(1 - \frac{\omega - \omega_\theta}{\omega_\theta} \sqrt{\frac{\Delta}{E_{Fl}}} \right) \right]^{1/2} \end{array} \right). \quad (26)$$

Here $\omega_\theta = \sqrt{2m^*s^2\Delta}/\hbar \sin \theta$ is the characteristic frequency of the maximum. For the nondegenerate (B) and degenerate (F) case we obtain

$$G_B = (n_l/\rho_{2D}k_B T_{el}) G(k_B T_{el}), \quad G_F = (2/\sqrt{\pi}) G(E_{Fl}), \quad (27)$$

where

$$G(E) = \frac{E_m}{4\sqrt{\pi}} \left(\frac{E_m}{2\pi\hbar s} \right)^2 \left(\frac{E_m \Delta z}{\hbar s} \right)^2 \left(\frac{T}{\Delta} \right)^2 \frac{\hbar}{E\tau_{da}(E)}. \quad (28)$$

Here $\rho_{2D} = m^*/\pi\hbar^2$ is the 2D density of states, $\rho_{2D}T_{el} > n_l$, and $\tau_{da}(E)$ is the relaxation time of 3D electrons scattered by equilibrium acoustic phonons in bulk semiconductor.¹² The appearance here of such bulk value is only a suitable characteristic of the electron-phonon interaction and is not connected with the physical processes discussed. We point out that (26) is obtained for $(\Delta/4k_B T_{el}) \gg 1$ in the nondegenerate case and for $\Delta \gg E_{Fl}$ in the degenerate case. As is seen from (26) in both cases the maximum corresponds to ω_θ and the half-width is equal to $\omega_\theta \sqrt{T_{el}/\Delta}$ in the former case and

to $\omega_\theta \sqrt{E_{Fl}/\Delta}$ in the latter. Using Eq. (26) and the results of Ref. 6 for $(\delta G)^{\text{intra}}$ we find, in the degenerate case, that the intrawell contribution can be neglected if the following condition is satisfied:

$$\frac{k_B^4 T_e^4 \sin^3 \theta}{4E_{Fl}E_m^3} \ll \frac{T^2}{\Delta^2} \{1 - \cos[\omega_\theta \Delta z \cos(\theta)/s]\}. \quad (29)$$

Thus the intrawell contribution can be neglected for strongly degenerate electrons and not too small tunneling matrix element T . The energy and angular dependences of $(\delta G)^{\text{inter}}$, calculated numerically using Eqs. (3), (8), and (21), differ considerably from the simple asymptotic result (26) because near the maximum of the ω dependent $(\delta G)^{\text{inter}}$ for optimal θ the factor (21) already oscillates and begins to decrease very strongly with increasing ω . As seen from Figs. 3 and 4, given for the degenerate case with $n_l = 1.24 \times 10^{11} \text{ cm}^{-2}$ and $E_{Fl} = 4 \text{ meV}$, $(\delta G)^{\text{inter}}$ is considerably different for different parameters of the DQW structure. This is related to the factor (21) which not only determines the position of the minima of the differential acoustic flow, determined generally by Δz , but also shifts the emission maximum approximately by a factor of 2 when d_l is halved. The maximum of the differential acoustic flow for diminishing QW widths, as seen from Figs. 3 and 4, becomes considerably larger due to increasing the factor ω^3 in (8) when the frequency at the maximum is doubled. Moreover, for smaller QW width the angular diagram of emission becomes narrower and the angle for which the differential acoustic flow has the largest value tends to be smaller.

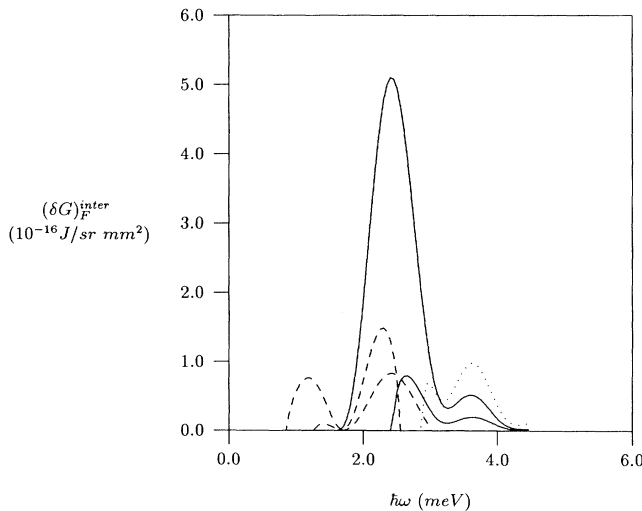


FIG. 3. Energy dependences of $(\delta G)_F^{\text{inter}}$ for the DQW structure with $d_l = 8.4 \text{ nm}$, $d_r = 10 \text{ nm}$, $d = 3 \text{ nm}$, and $U = 300 \text{ meV}$; $\theta = 4.5^\circ$ (dotted curve), $\theta = 9^\circ$ (solid curves), $\theta = 18^\circ$ (dashed curves). The upper dotted, solid, and dashed curves correspond to $\Delta = 10 \text{ meV}$ and the corresponding lower curves to $\Delta = 20 \text{ meV}$. In the units shown the lower dotted curve coincides with the horizontal axis.

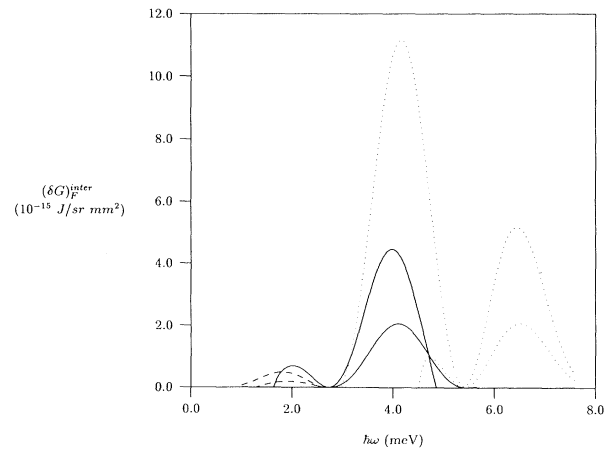


FIG. 4. Energy dependences of $(\delta G)_F^{\text{inter}}$ for the DQW structure with $d_l = 4.2 \text{ nm}$, $d_r = 4.4 \text{ nm}$, $d = 3 \text{ nm}$, and $U = 870 \text{ meV}$; other notations coincide with those in Fig. 3.

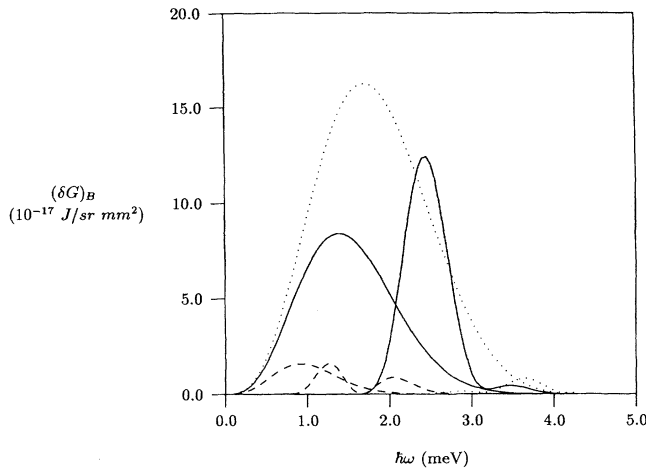


FIG. 5. Energy dependences of differential acoustic flows δG for nondegenerate electrons in a DQW structure with $d_l = 9$ nm, $d_r = 10$ nm, $d = 3$ nm, and $U = 300$ meV; $\Delta = 10$ meV; $\theta = 4.5^\circ$ (dotted curves), $\theta = 9^\circ$ (solid curves), $\theta = 18^\circ$ (dashed curves). In each set of curves the rightmost curve is for interwell transitions and the leftmost curve for intrawell transitions.

In Fig. 5 we plot the energy dependences of interwell and intrawell differential acoustic flow for nondegenerate electrons at temperature $k_B T_e = 1$ meV and with density $n_l = 2.5 \times 10^{10}$ cm $^{-2}$. The dotted, solid, and dashed curves correspond to $\theta = 4.5^\circ, 9^\circ$, and 18° , respectively, and the other parameters are specified in the caption. The intrawell contribution from the r QW is neglected since we assume $n_l \geq n_r$. As can be seen, the energy and angular dependences for the interwell contribution are similar to those discussed above for the degenerate case, compared with curves for $\Delta = 10$ meV in Fig. 3. The smaller typical values of the intensity here are mainly due to the smaller electron concentrations. As for the intrawell contribution from the l QW, the corresponding maximum value, for given θ , is often comparable with that of the interwell contribution for the same θ . However, the phonon energies corresponding to two such maxima are appreciably shifted with respect to each other.

The numerical results represented in Fig. 5 correspond to $n_l \geq n_r$ and $T_{el} \geq T_{er}$. This could be realized in the regime of photoexcitation or of modulation of the transverse voltage, i.e., in cases (i) and (iii) as mentioned in Sec. I. The simplest and easiest to realize experimentally nonequilibrium situation is heating by a longitudinal electric field, case (ii) in Sec. I. In this case the concentrations n_l and n_r are related by the barometric factor, i.e., $n_l/n_r \propto \exp(-\Delta_T/k_B T_e)$, if the heating is controlled by electron-electron scattering. The interwell contribution could be observed in such a case for not too large values of $\Delta_T/k_B T_e$, when it is necessary to consider both the transitions from the l to the r QW and the reverse ones. Numerical results for this case, which take into account both transitions for interwell contributions and intrawell contributions, are shown in Fig. 6 for a DQW structure

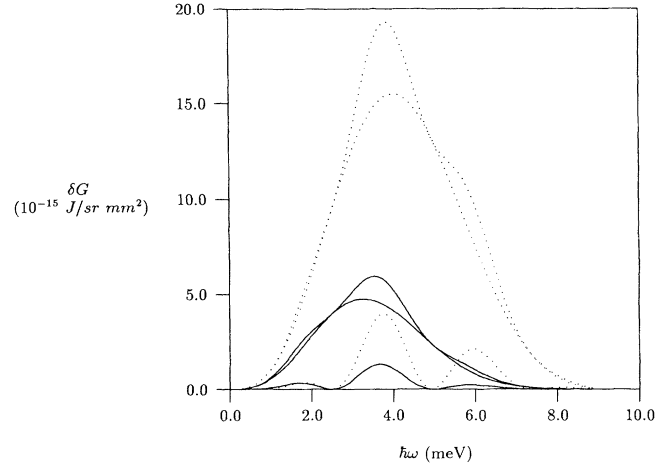


FIG. 6. Energy dependences of differential acoustic flows δG for heated nondegenerate electrons in a DQW structure with $d_l = d_r = 4.2$ nm, $d = 3.8$ nm, $U = 870$ meV for $\theta = 4.5^\circ$ (dotted curves), and $\theta = 9^\circ$ (solid curves). In each set of curves, at $\hbar\omega = 4$ meV, the lowest one is for interwell and the next one for intrawell transitions; the highest curve is the total contribution.

with $\Delta_T \cong 5.0$ meV and $T \cong 1.5$ meV. In addition, we show the results corresponding to a transverse voltage for $\Delta = 4$ meV and $k_B T_e = 5$ meV. The total concentration is $n_l + n_r = 1.7 \times 10^{11}$ cm $^{-2}$ and the marking of the curves is the same as that in Fig. 5. The character of the interwell contribution is analogous to that shown in Fig. 4 for the degenerate case with similar parameters for the DQW structure; this contribution substantially modifies the form of the total energy dependence of δG .

V. ANGULAR DEPENDENCES OF EMISSION INTENSITY AND TOTAL ACOUSTIC ENERGY FLOW

We now consider the emission intensity from a DQW, i.e., the differential acoustic flow integrated over frequency, determined by Eq. (9), that depends only on the polar angle θ . Integrating δG , given by Eq. (26), over frequency for the case of large angles [determined by inequalities (23) and (24)], we obtain a simple angular dependence of the emission intensity

$$\left[\frac{dG}{d\Omega} \right]_{F,B}^{\text{inter}} = \frac{\sqrt{\pi} E_m \cos^2 \theta}{\hbar \sin^7 \theta} \left(\frac{\sqrt{\pi} G_F \sqrt{E_{Fl}/\Delta}}{G_B \sqrt{T_{el}/\Delta}} \right). \quad (30)$$

Here, in comparison with Eq. (26), an additional factor $1/\sin \theta$ appears because the width of the peak is proportional to ω_θ . With increasing θ Eq. (30) shows that the emission intensity decreases monotonically with θ . For the reverse inequality sign in Eq. (23), i.e., for asymptotically small angles, $dG/d\Omega$ tends to zero for $\theta \rightarrow 0$, because in such a case only "vertical" transitions, such as transition 1 in Fig. 1, are allowed. Hence, the maxi-

imum of the emission intensity $dG/d\Omega$ is at optimal polar angle θ_0 , the order of which could be estimated for different cases (see Ref. 13). However, due to the complicated angular dependence of the factor (21) the exact value of θ_0 can be obtained only numerically from the calculation of the angular distribution of the emission intensity. The dependence of θ_0 on Δ and on the widths of the QW's (cf. Ref. 13) and also the dependence of $dG/d\Omega$ on θ for small angles, of the order of θ_0 , are illustrated in Fig. 7. The curves are obtained with the parameters of Fig. 3 (wide QW's) and of Fig. 4 (narrow QW's) for $E_{Fl} = 4$ meV.

The peak form of $dG/d\Omega$ for nondegenerate electrons represented in Fig. 5 is analogous to that given in Fig. 7 for degenerate electrons. The $dG/d\Omega$ dependences for heating by the longitudinal electric field are given in Fig. 8 (the differential acoustic flow in this case is represented in Fig. 6). Here it is necessary to take into account all intrawell and interwell contributions. The interwell contribution could be distinguished using the dependence of the curves for $dG/d\Omega$ on the energy splitting Δ_T , which can be controlled by a transverse voltage. From the normalized curves in Fig. 8 it is seen that with increasing Δ (and hence Δ_T) we have not only a decrease in the maximum values of the emission intensity (these values are given in the caption) but also a substantially larger decrease of the intensity for small angles because of depopulation of the l QW. This is related mainly to the interwell contribution to the emission. Then taking into account the dependence of the $dG/d\Omega$ curves on Δ , we can single out the interwell contribution because the form of curves for the intrawell contribution is independent of Δ .

The dependence of the total acoustic energy flow G_z , determined by formula (12), on Δ changes with the geometry of the DQW structure for degenerate electrons; when

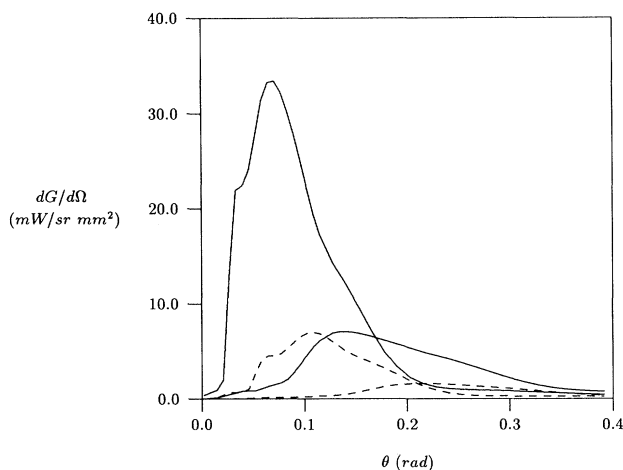


FIG. 7. Angular dependences of the emission intensity $dG/d\Omega$ for the DQW structure. At $\theta = 0.15$ rad, the first and third curves are obtained with the parameters of Fig. 3 (here $10 dG/d\omega$ is plotted), the second and fourth ones with those of Fig. 4. Solid curves: $\Delta = 10$ meV; dashed curves: $\Delta = 20$ meV.

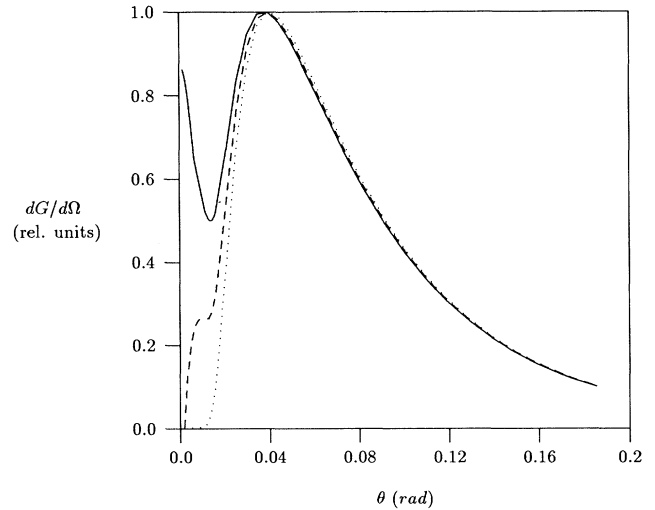


FIG. 8. Angular dependences of the normalized emission intensity $dG/d\Omega$ for the DQW structure with the same parameters as in Fig. 6. Solid curve: $\Delta = 2$ meV, $\max[dG/d\Omega] = 218$ mW/sr mm²; dashed curve: $\Delta = 4$ meV, $\max[dG/d\Omega] = 174$ mW/sr mm²; dotted curve: $\Delta = 10$ meV, $\max[dG/d\Omega] = 126$ mW/sr mm². The curve for $\Delta = 20$ meV is indistinguishable from the dotted one. All interwell and intrawell contributions have been taken into account.

the typical width of the structure is reduced (for fixed barrier width) the total acoustic energy flow increases appreciably in analogy with the differential acoustic flow discussed in Sec. IV. The same holds for nondegenerate electrons when T_e changes. From Fig. 9 it is seen that with increasing Δ the value of G_z is diminished. This is related to the reduction of the factor determined by Eqs. (21) and (25) for the two curves in Fig. 9 corresponding to the degenerate case; both curves tend to zero. Here the tunnel matrix element $T \cong 3.4$ meV for a structure

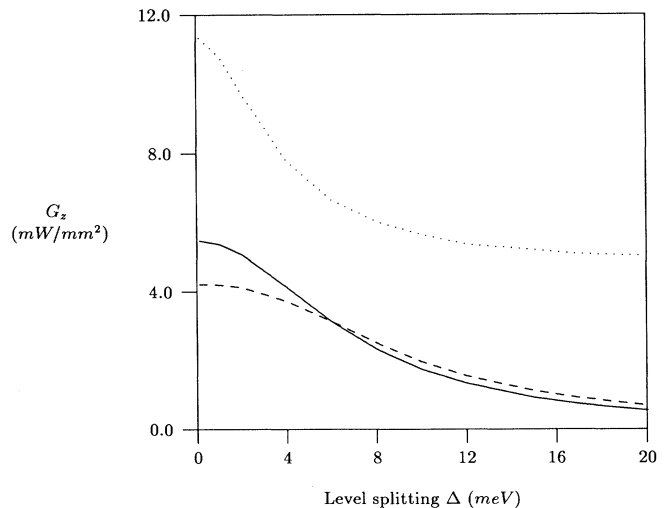


FIG. 9. Total acoustic energy flow G_z as a function of Δ corresponding to Fig. 3 (solid curve; here $10G_z$ is plotted), Fig. 4 (dashed curve), and Fig. 6 (dotted curve).

with wide QW's and $k_B T \cong 3.9$ meV for a structure with narrow QW's. In the nondegenerate case with increasing Δ the result tends to the intrawell contribution only from the r QW as is seen from the third curve in Fig. 9. After subtracting the intrawell contribution we can estimate that the interwell one amounts to more than 10% of G_z for $\Delta \leq 4$ meV and more than 20% for $\Delta \leq 2$ meV.

VI. DISCUSSION AND CONCLUDING REMARKS

Here we discuss the assumptions and carry out some estimations of the phonon energy flow caused by interwell tunnel transitions. The considerations given above show that there is a considerable difference between the characteristics of the acoustic phonons emitted during interwell and intrawell transitions. This is due to an interwell interference which changes qualitatively the energy and angular dependences of δG . It thus gives the possibility of distinguishing the interwell channel of acoustic-phonon emission. The numerical results of the paper show the possibility of using such a process for the generation of high-energy phonons. This can be realized if several conditions hold; a more detailed description of this case demands more precision in the model under consideration.

An extension of the model introduced in Secs. II and III is connected with (a) the necessity of a self-consistent determination of the electron energy spectrum since for high electron concentrations substantial transverse electric fields are possible; (b) modification of bulk phonon modes if the DQW layer is near the surface of the sample; (c) taking into account the piezoelectric electron-phonon

interaction which, because it decreases with increasing transmitted momentum, could give a contribution to the low-energy wing of the considered distributions. Further, it has been assumed that other processes of the nonequilibrium electron relaxation in the DQW structure are ineffective in comparison with the acoustic channel. This corresponds to small electron concentration in the structure so that their Coulomb relaxation (similar to an Auger process) is ineffective and to the case of $\Delta < \hbar\omega_0$ when optical-phonon emission is negligible (for $\Delta > \hbar\omega_0$ generated optical phonons are decomposed in pairs of acoustic phonons that change the distribution of the latter). It should be pointed out that the approximations of our treatment are further connected with the neglect of phonon absorption in the boundary condition (2). However, the above-mentioned possible extensions do not substantially change the results of this paper, e.g., the typical value of the interwell differential acoustic flow as well as its energy and angular dependences. Our results show an appreciable contribution of the interwell channel of acoustic-phonon emission in comparison with values typical for the intrawell channel.¹⁴ Thus, the observation of this contribution is possible in a variety of cases, mentioned in Sec. I, characterized by a nonequilibrium electron occupation in DQW structures.

ACKNOWLEDGMENTS

The work of F.T.V. and O.G.B. was supported by Fundamental Research Fund of Ukraine. P.V. acknowledges the support of NSERC Grant No. OGPC121756.

¹A. M. Chin, V. Narayanamurti, H. L. Stormer, and A. C. Gossard, in *Proceedings of the 17th International Conference on the Physics of Semiconductors*, edited by J. D. Chadi and W. A. Harrison (Springer-Verlag, New York, 1985), p. 333.
²M. Rosenfusser, L. Koster, and W. Dietsche, *Phys. Rev. B* **34**, 5518 (1986).
³L. J. Challis, A. J. Kent, and V. W. Rampton, *Semicond. Sci. Technol.* **5**, 1179 (1990).
⁴B. Vinter and A. Tardella, *Appl. Phys. Lett.* **50**, 410 (1987).
⁵B. Deveaud, A. Chomette, F. Clerot, P. Auvray, A. Regreny, R. Ferrera, and G. Bastard, *Phys. Rev. B* **42**, 7015 (1990).
⁶F. T. Vasko, *Fiz. Tverd. Tela (Leningrad)* **30**, 2092 (1988) [*Sov. Phys. Solid State* **30**, 1207 (1988)].
⁷A. Yariv, C. Lindsey, and U. Sivan, *J. Appl. Phys.* **58**, 3669 (1985).

⁸F. T. Vasko, *Fiz. Tekh. Poluprovodn.* **26**, 825 (1992) [*Sov. Phys. Semicond.* **26**, 464 (1992)].

⁹V. L. Gurevich, *Transport in Phonon Systems* (North-Holland, New York, 1986).

¹⁰P. J. Price, *Ann. Phys.* **133**, 217 (1981).

¹¹More suitable asymptotic expressions, for comparison with the results of the numerical calculations given, e.g., in Fig. 3, could be obtained by substituting in Eqs. (25) and (26) the factor $[1 - \cos(q_z \Delta z)]$ instead of the factor $(q_z \Delta z)^2/2$. Then in Eq. (25) we can take $q_z d_{l,r} \approx 1$.

¹²K. Seeger, *Semiconductor Physics: An Introduction* (Springer-Verlag, New York, 1991).

¹³Taking into account the result of Ref. 11 for θ_0 we obtain $\theta_0 \approx [d_l \sqrt{m^* \Delta T}] / (\sqrt{2\pi\hbar})$.

¹⁴G. A. Toombs, F. W. Sheard, D. Nelson, and L. J. Challis, *Solid State Commun.* **64**, 577 (1987).